

# Signal Distortion in Coaxial Transmission Lines: Application to Logic Pulses, Photomultiplier Pulses, and Fast Current Transformer Signals

A. Reiter, O. Chorniy  
Beam Instrumentation Department

June 21, 2016

## 1 Introduction

This short application note describes the distortion of fast signals in coaxial transmission lines. Here, by "fast" pulses we intend pulses of durations below  $1 \mu\text{s}$ .

Typical "standard" pulse shapes - logic pulses and photomultiplier pulses - have been considered. However, distortion calculations with smooth input signals cannot answer intuitively a very fundamental question: When is a "significant structure" or sub-structure of a signal destroyed by the cable response?

Therefore, a practical approach was chosen for the judgement of cable performance. A "bad" transformer signal served as reference for calculations because the chosen signal contained structures of various duration, including spikes, and showed undesired ringing effects. The simulations were completed by measurements of the signal distortion in Flexwell and Andrew Heliax coaxial cables.

## 2 Calculation of Signal Distortion

An excellent treatment of the subject can be found in reference [1]. The calculations follow the prescription of reference [2]. Some of the data presented therein was reproduced to confirm the validity of the software implementation in Python.

### 2.1 Comparison to CLAS-NOTE

Figures 1, 2 and 3 attempt to reproduce Figures 2, 3, and 7 of reference [2] using the cable parameters stated therein. Parameters for other cables, air-filled cables of different diameter, ECO393 or Andrew FSJ1RN-50B, have been extracted from fits to attenuation values taken from data sheets. The latter two cable types are commonly used at GSI.

## 2.2 Signal Distortion of Standard Pulses

Figures 4, 5 and 6 show the predicted signal distortions for a 20 ns long photomultiplier pulse and NIM pulses of 10 ns and 50 ns length. Distortions were calculated for nine different cables: low-distortion air-filled coaxial cables; well known standard cables like RG 213, RG 58 or RG 174; and a CAT7 network cable.

The various cables can be grouped according to their performance:

- RG 174
- RG 58, CAT7
- RG 213, Andrew Heliax FSJ1RN, Belden 9913, ECO 393
- Air-filled 1/2 and 7/8 inch

It may be interesting to note that the CAT7 cable has a similar performance as the RG 58 cable.

## 2.3 Signal Distortion of FCT Pulse

As discussed in the introduction, a "bad" FCT signal was chosen as reference for calculations due to its different types of structures. The 12-bit ADC of the acquisition system was sampling at a rate of 1 GSa/s. Although the measured signal of the FCT installed at the HTP beam line had passed through about 90 m of RG 213 cable, it is composed of a stack of three broader distributions (650 ns, 300 ns and 100 ns) and contains fast spikes (ringing). Hence, for transmission of up to 100 m such a cable seems a reasonable choice.

### 2.3.1 Calculated Distortion

Figure 7 and Figure 8 show this reference pulse (blue trace) together with the expected signal shapes after 200 m long coaxial cables Andrew Heliax, as a representative of the 2nd best cable class (green), and the two air-filled cables of the top class (light blue and red). The two figures show the same data on different time scales. The Andrew Heliax cable is not able to preserve very fast structures as the ringing is almost completely washed out, e.g. in the tail of the pulse in Figure 8(bottom). This is not the case for the two air-filled cables which both reprocude the original signal structures. The signal quality for the larger cables is only slightly better compared to the smaller cable. Therefore, the 1/2 inch cable seems to be the most appropriate choice.

### 2.3.2 Measured Distortion

The signal distortion in a 100 m long 3/8 inch air-filled Flexwell coaxial cable was measured in the laboratory using an arbitrary function generator Tektronix AFG 3102 (1 GSa/s, 100 MHz bandwidth) and a Tektronix DPO 2042 oscilloscope (1 GSa/s, 200 MHz). The results are shown in Figures 9 and 10. The measurement confirms the

previous conclusion, although this cable does not reach the performance of the two simulated air-filled cables.

## 2.4 "Direct" Unfolding and Noise

At the CNAO facility the signal distortion by a 75 m long Andrew cable has been measured with a 5 GSa/s digital oscilloscope of 1 GHz bandwidth. Data sets were recorded for two pulse shapes, a 10 ns long triangular pulse and a 30 ns long square pulse. In Figure 11 and Figure 12 the input pulse is shown as blue trace, the distorted pulse as green trace. The trace in red color in left and right plot of each figure represent, respectively:

- the case where the input pulse (blue) was folded with the cable response to yield the distorted pulse (green):  $\text{red} = \text{IRFFT} ( \text{RFFT}(\text{blue}) * \exp(-\alpha L) )$
- the case where the distorted pulse (green) was unfolded with the cable response to yield the input pulse (blue):  $\text{red} = \text{IRFFT} ( \text{RFFT}(\text{green}) * \exp(+\alpha L) )$

Here, RFFT is the real fourier transformation and IRFFT the inverse operation, while  $\alpha$  represents the frequency-dependent attenuation coefficient and L the cable length. The calculated signal shapes agree well with the measured data, but in the case of "direct" unfolding the noise level is significantly increased. This noise level can be reduced in a second step by a smoothing algorithm or a priori by selection of a more elaborate unfolding procedure.

## 3 FCT: Electronics and Acquisition

### 3.1 Electronics Chain at HTP

The reference pulse was measured in the high-energy beam line HTP. The electronics chain for this FCT is composed of:

- Tunnel hardware: GSI-type FCT and remote-controlled attenuator (3 dB insertion loss, 0-63 dB attenuation) which is followed by a fixed-gain amplifier unit (gain=45.2 dB, 0.3-500 MHz BW, NF= 1.15 db, 1 dB compression point 11 dBm)
- Signal transmission: coaxial cable (87 m RG 213, <10 m RG 174)
- Acquisition hardware: Fast sampling ADC (1 GSa/s, 12 nominal bit)

A similar scheme will likely be implemented in the new facility, but for the long distance transmission a coaxial cable or an optical link are viable options.

	Attenuator	Amplifier	Optical Link
Model	MTS T-PAS-1000/63-5401	Miteq 1423U	point2point PAT-K1-6H + PAR-K1-6R
Bandwidth [MHz]	DC - 1000	0.3 - 500	0.002 - 1350
Insertion loss [dB]	-(2-3)	0	-(1-3)
Att./gain [dB]	-63 - 0	45.2	0
Comp. point [dB]	—	11	>0
V(pp) [mV]	—	2244	632
Input P3 [dBm]	—	~(11+10)	>10
Noise figure	—	1.15	24
Equiv. RMS input noise [mV]	—	0.011	0.26 (1300 MHz) 0.16 (500 MHz)
RMS output noise [mV]	—	2.1	0.26
MDS [dBm]	—	-85.9	-58.9
DR [dB]	—	97.9	57.9
SFDR [dB]	—	71.1	39.3

### 3.2 Optical Link

The optical link by PPM consisting of transmitter PAT-K1-6H and receiver PAR-K1-6R has a bandwidth between 2 kHz and 1.35 GHz, 2 dB insertion loss, 0 dBm compression point,  $IP1 = 10$  dBm, and a noise figure  $NF = 24$  dB. The spurious free dynamic range SFDR is about 40 dB. The cost for the optical link without fibre is about 5600 Euro (prices taken from offer by EMCO in 12/2012). The optical link introduces active components in the tunnel and requires remote control by the DAQ system to enable/disable the transmitter. It therefore increases system complexity. Further, disconnecting and reconnecting the fibre at transmitter or receiver has been observed to change the insertion loss significantly (only crucial, if the bunch charge is measured).

Key parameters of attenuator module, amplifier and optical link are summarised in tabular form.

### 3.3 Noise Figure and Dynamic Range

If we disregard the attenuator as noise source (justified, if the attenuator output signal is within the dynamic range of the following amplifier), the noise figure of the amplifier/optical link stage is  $NF(att/opt.) = 1.2$  dB and only slightly higher due to the large gain of the first stage.

Assuming 1300 MHz BW the 24 dB noise figure of the optical link corresponds to a minimum-detectable signal MDS of -58.9 dBm or 0.26 mV(rms) noise level. See Figure 13 which shows the pulse response and baseline noise of the optical link. At 500 MHz BW the amplifier input noise is 11.5  $\mu$ V(rms) which translates to 2.1 mV(rms) noise level

at the output. If we combine these RMS values in quadrature, one obtains a total RMS value of 2.12 mV(rms). This corresponds to a noise factor of 1.0076 or a noise figure NF=1.26 dB. This estimate is slightly higher than the 1.2 dB calculated for the cascade.

We consider a signal acquisition in an ADC with following parameters: symmetric +/-1 Volt input range, fixed centered baseline and 10/12 nominal bits. The ADC granularity is then  $\sim 2.0/0.5$  mV/channel. Therefore, a 10 bit ADC seems not appropriate since the output noise of the FCT electronics is 2.1 mV(rms) and one typically must subtract 2 bits from the nominal value to obtain the effective number of bits. If we select a 12 bit ADC and assume 10 effective bits, its dynamic range is 62 dB for the symmetric voltage input range. For unipolar FCT pulses the dynamic range is reduced to 55.9 dB as one effective bit is lost.

The optical link would be the limiting element of the dynamic range and reduce it to 40 dB which is significantly lower than the DR of amplifier and ADC units.

## 4 Conclusion

The signal distortion of photomultiplier pulses and logic NIM pulses have been calculated for three cable lengths of 50 m, 100 m and 200 m which are thought to represent "typical" length for installations in the GSI/FAIR facility. The theoretical calculations have been verified by a measurement with two different coaxial cable types.

The signal transmission of fast current transformer signals has been discussed for coaxial cables and an optical link. For cable lengths below 250 m air-filled coaxial cables seem a more appropriate choice compared to an optical link which offers negligible signal distortion at the expense of dynamic range.

We also point out that the CAT7 network cable performs not much worse than the commonly used RG 58 cable. Hence, it may serve for the transmission of more than one signal in dedicated applications.

## References

- [1] E.S. Smith, *Dispersion in Commonly Use Cables*, CLAS-NOTE-91-007
- [2] R.L. Wingington and N.S. Nahman, *Transient Analysis of Coaxial Cables Considering Skin Effect*, Proc. of the IRE, February 1957

## List of Figures

1	Signal distortion of 10 ns logic pulse in 100m cable Belden 9913. . . . .	7
2	Signal distortion of 10 ns NIM pulse in cables and 300 ns propagation delay. Cable lengths are stated in the legend. . . . .	7
3	Signal distortion of photomultiplier pulse in cables of 50 m length. Cable types are stated in the legend. . . . .	8
4	Signal distortion of photomultiplier pulse in cables of 50 m, 100 m , and 200 m length. Cable types are stated in the legend. . . . .	9
5	Signal distortion of 10 ns NIM pulse in cables of 50 m, 100 m, and 200 m length. Cable types are stated in the legend. . . . .	10
6	Signal distortion of 50 ns NIM pulse cables of 50 m, 100m, and 200 m length. Cable types are stated in the legend. . . . .	11
7	Signal distortion of FCT signal in 50 m, 100 m, and 200 m long coaxial cables. A signal of HTPDT1, a GSI type transformer, measured after fast extraction of a single-bunch (h=1) served as reference data set because it shows a variety of sharp spikes on top of a stack of three broader structures of 650 ns, 300 ns and 100 ns length. . . . .	12
8	Data for 200 m long cables in Fig. 7 (bottom) for three time intervals. . .	13
9	Measured signal distortion in a 100 m long Flexwell coaxial cable. . . .	14
10	Data for 100 m long cable in Fig. 9 (bottom) for three time intervals. The offset in the two curves is due to the shift in the trigger timing. . . . .	15
11	Signal distortion of a 10 ns triangular pulse in Andrew Heliax of 75 m length. Blue trace: pulser signal; green trace: signal at end of transmission line; Red trace: calculated signal by folding (left) the undistorted pulse and unfolding (right) the distorted pulse with the cable response. . . . .	16
12	Signal distortion of a 30 ns triangular pulse in Andrew Heliax of 75 m length. Blue trace: pulser signal; green trace: signal at end of transmission line; Red trace:calculated signal by folding (left) the undistorted pulse and unfolding (right) the distorted pulse with the cable response. . . . .	16
13	Test of optical link for regular and minimum input voltages. Red = Input pulse to Transmitter; Blue = Output pulse at Receiver. The noise level of the output baseline is about 1.5 mV peak-peak or 0.3 mV(rms). . . . .	17

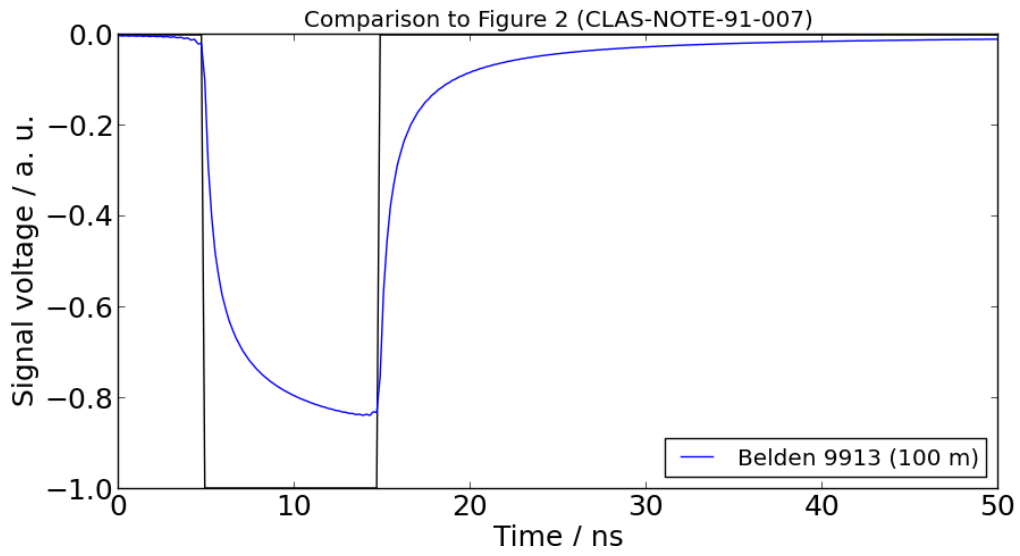


Figure 1: Signal distortion of 10 ns logic pulse in 100m cable Belden 9913.

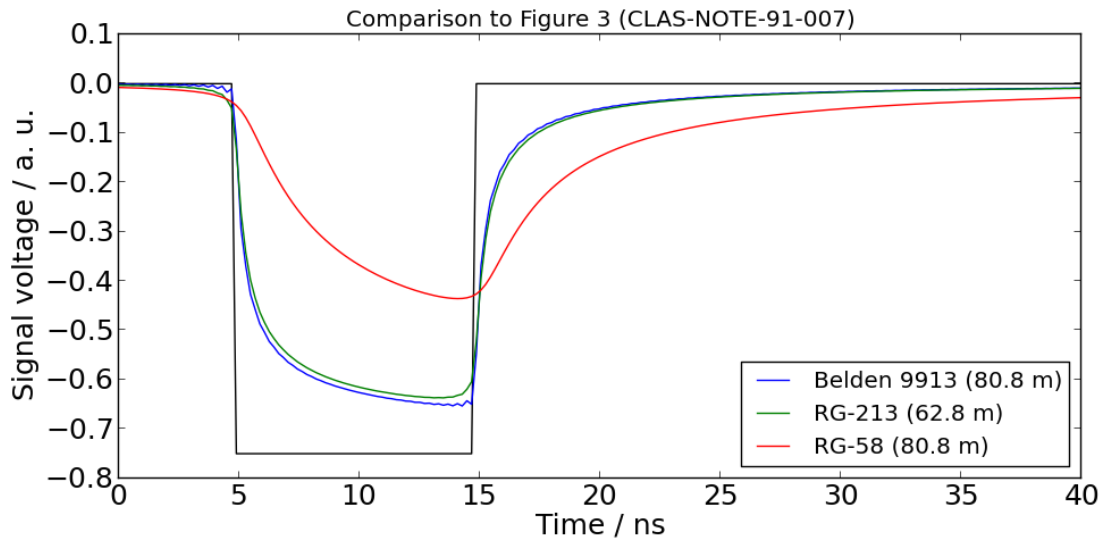


Figure 2: Signal distortion of 10 ns NIM pulse in cables and 300 ns propagation delay. Cable lengths are stated in the legend.

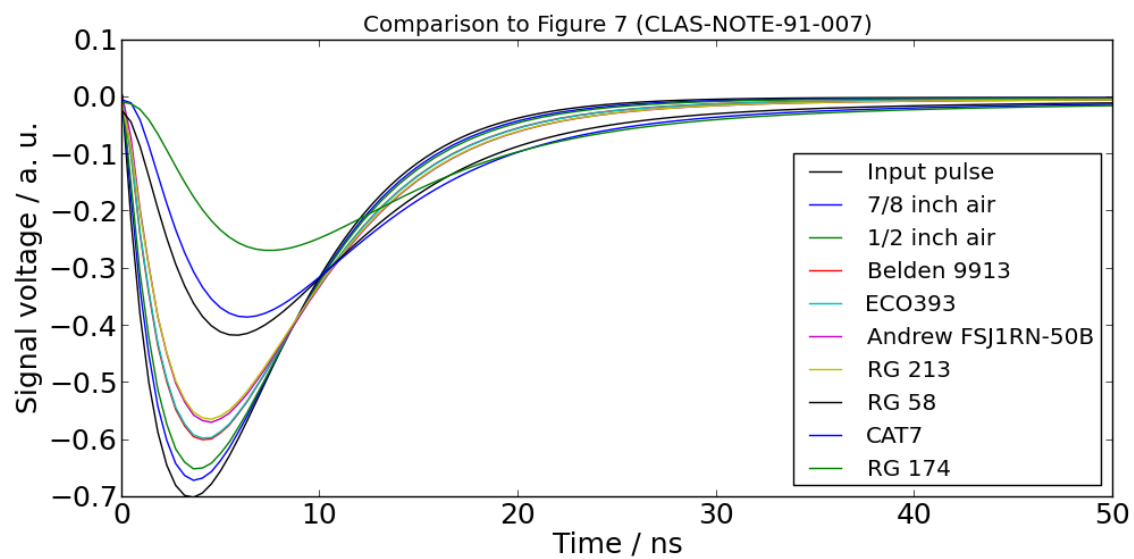


Figure 3: Signal distortion of photomultiplier pulse in cables of 50 m length. Cable types are stated in the legend.



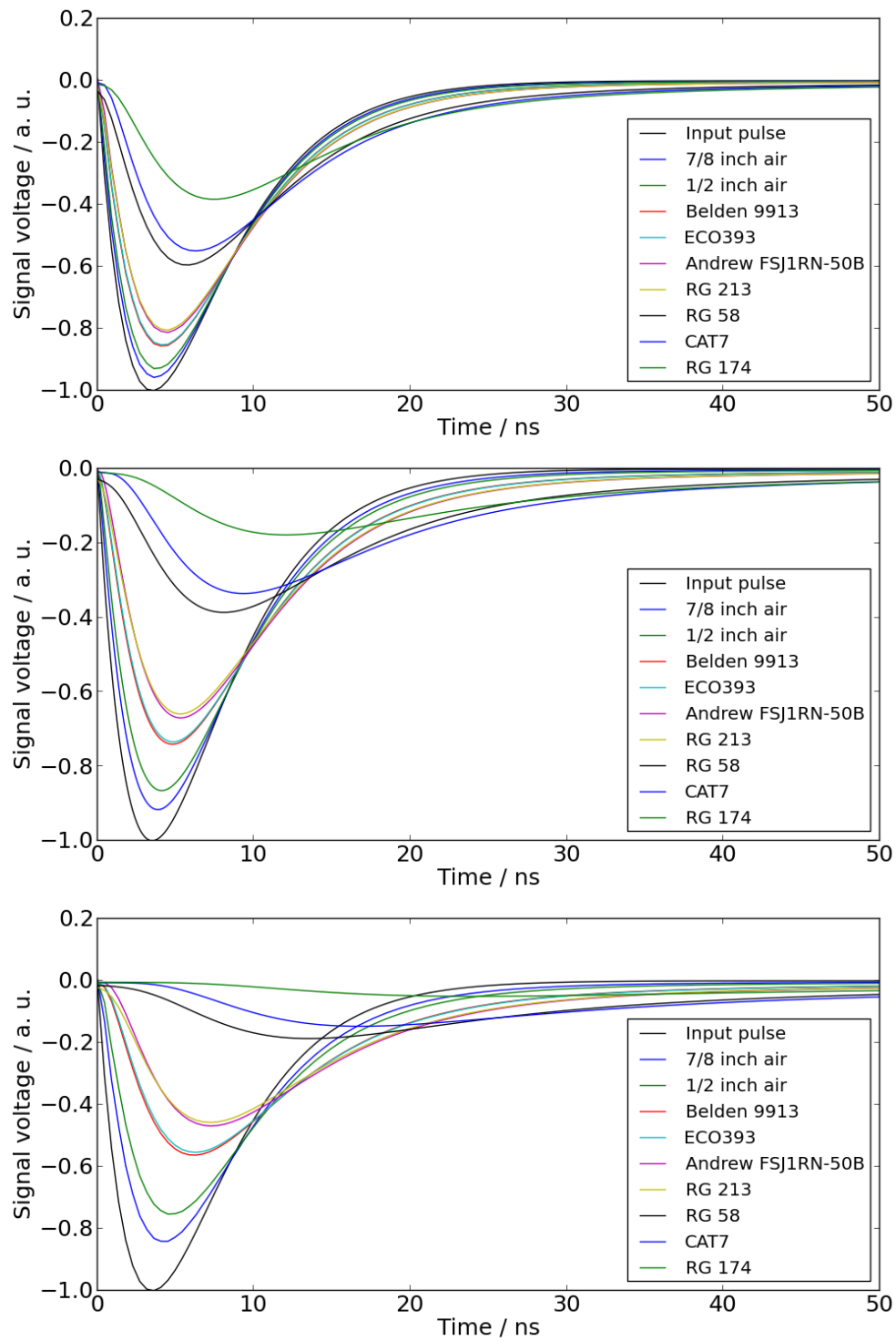


Figure 4: Signal distortion of photomultiplier pulse in cables of 50 m, 100 m , and 200 m length. Cable types are stated in the legend.

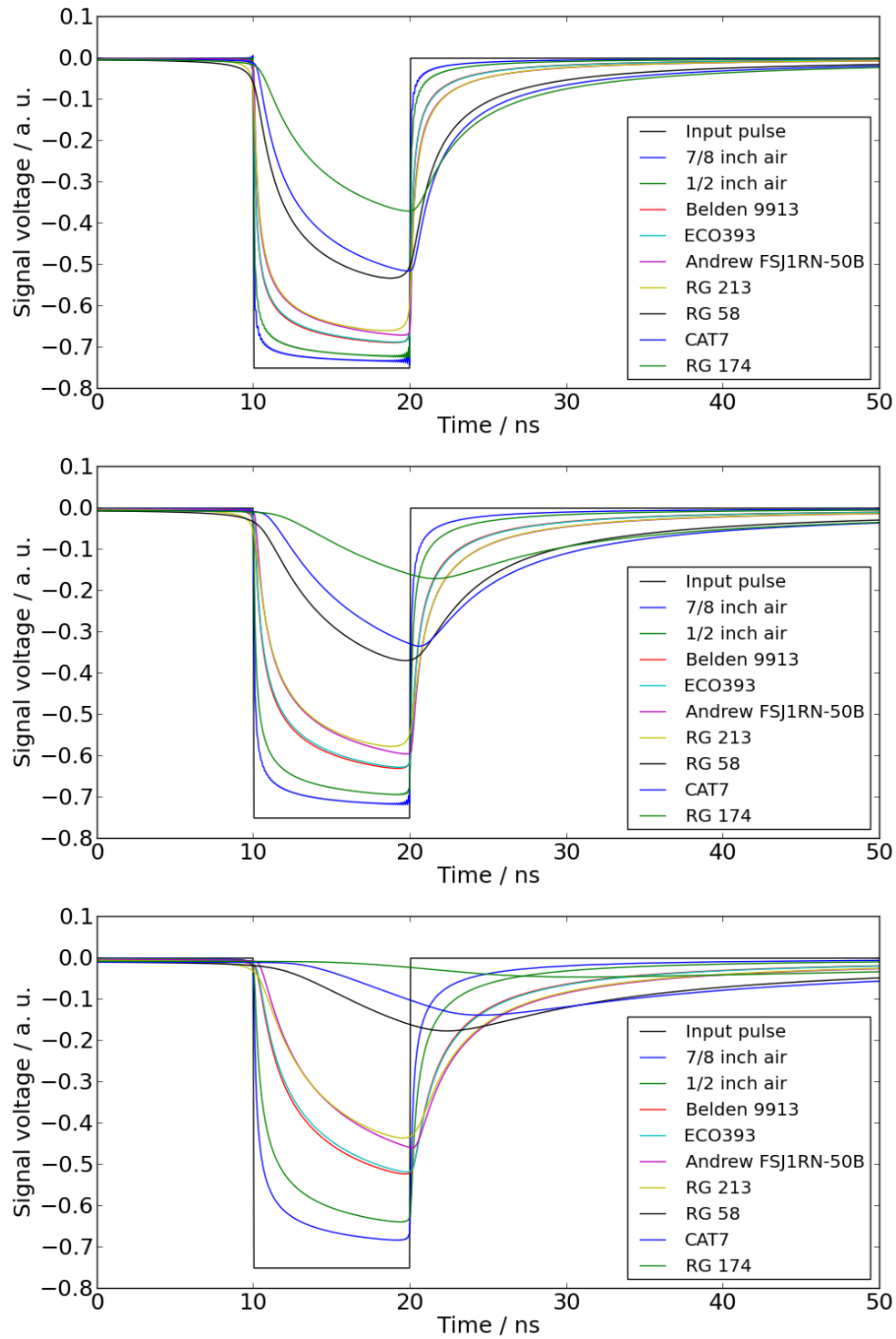


Figure 5: Signal distortion of 10 ns NIM pulse in cables of 50 m, 100 m, and 200 m length. Cable types are stated in the legend.

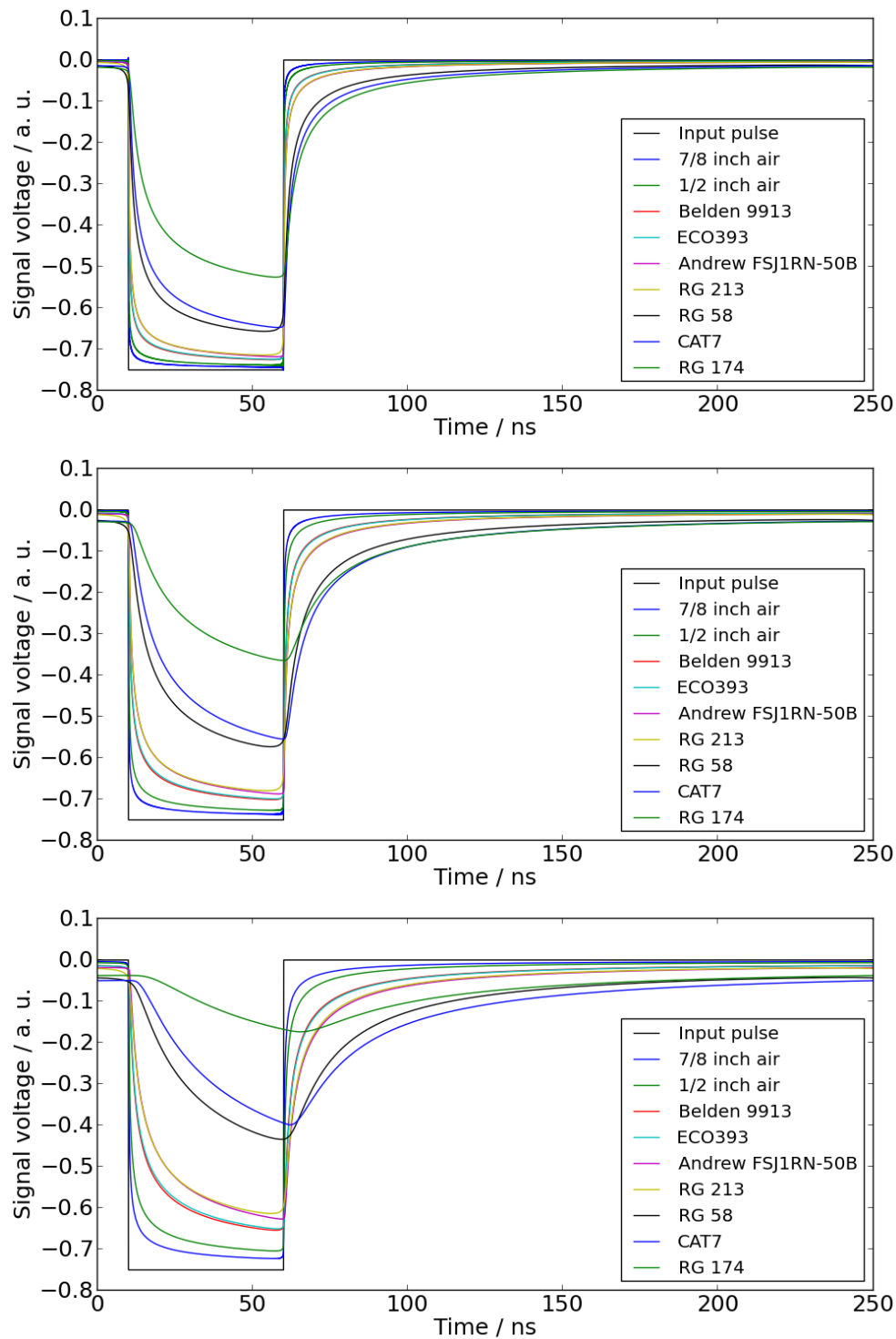


Figure 6: Signal distortion of 50 ns NIM pulse cables of 50 m, 100m, and 200 m length. Cable types are stated in the legend.

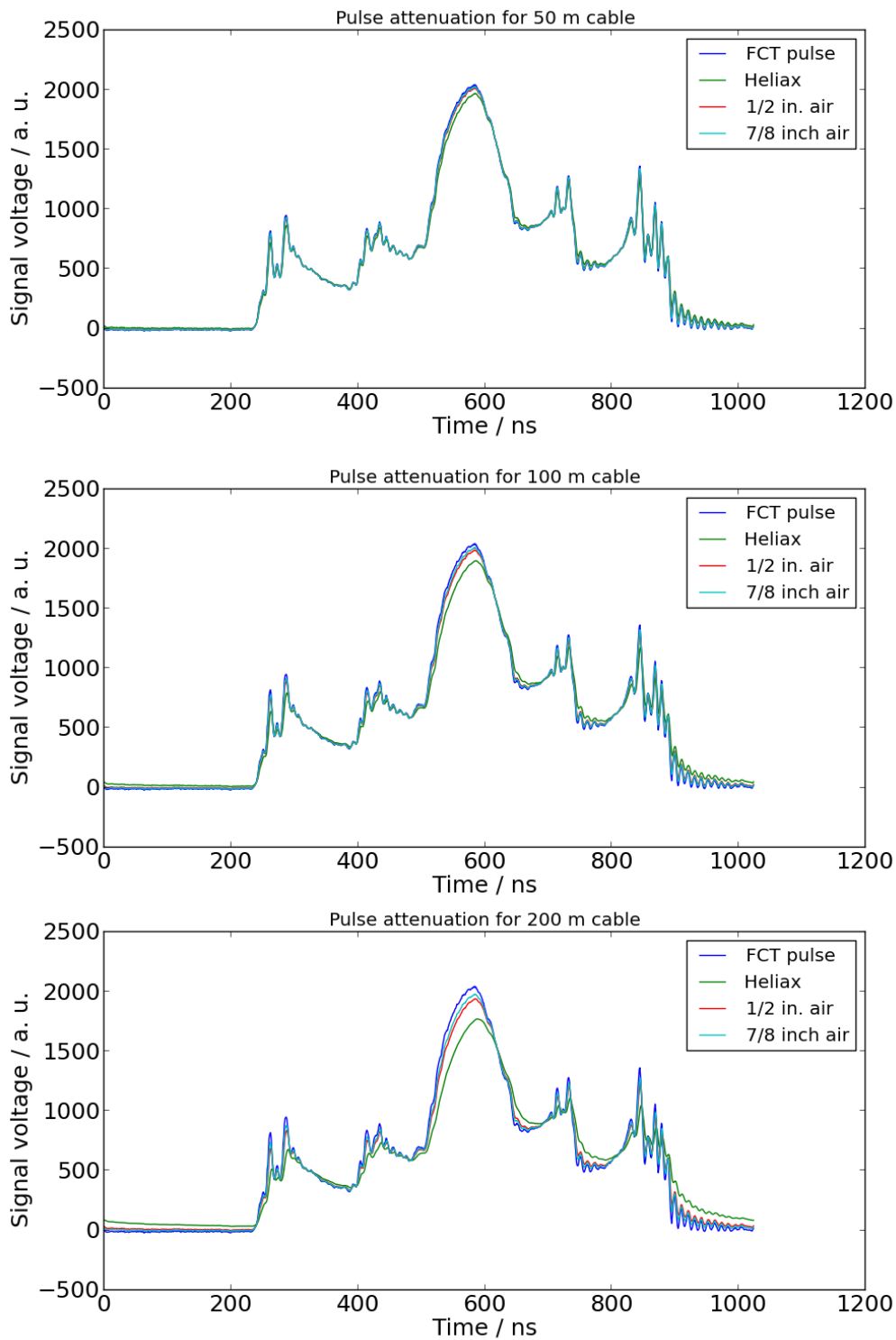


Figure 7: Signal distortion of FCT signal in 50 m, 100 m, and 200 m long coaxial cables. A signal of HTPDT1, a GSI type transformer, measured after fast extraction of a single-bunch ( $h=1$ ) served as reference data set because it shows a variety of sharp spikes on top of a stack of three broader structures of 650 ns, 300 ns and 100 ns length.

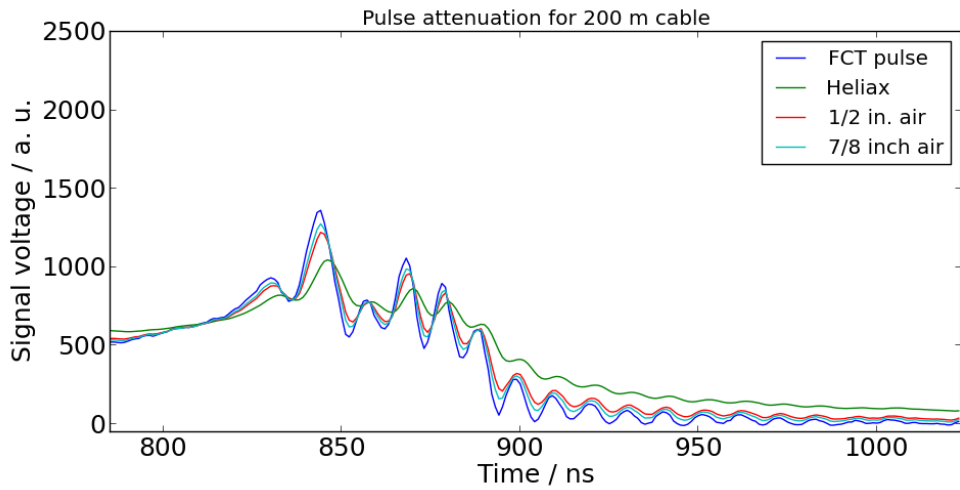
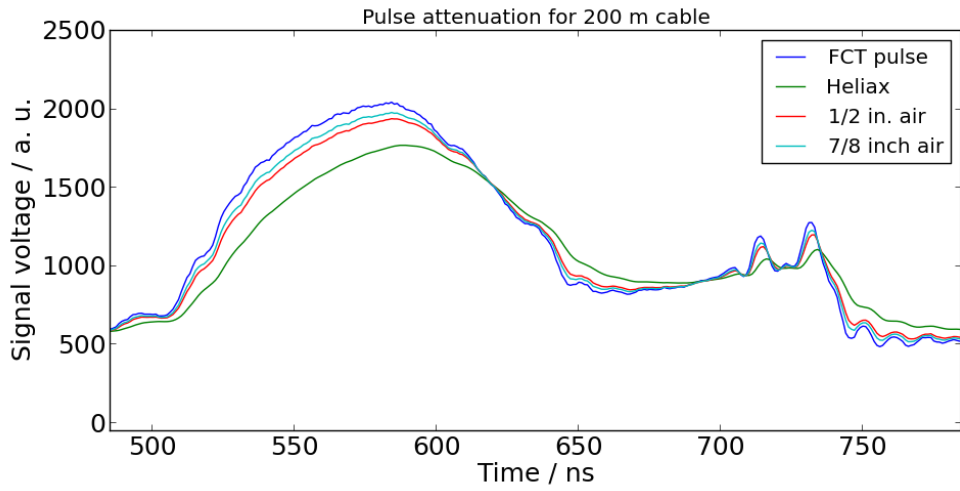
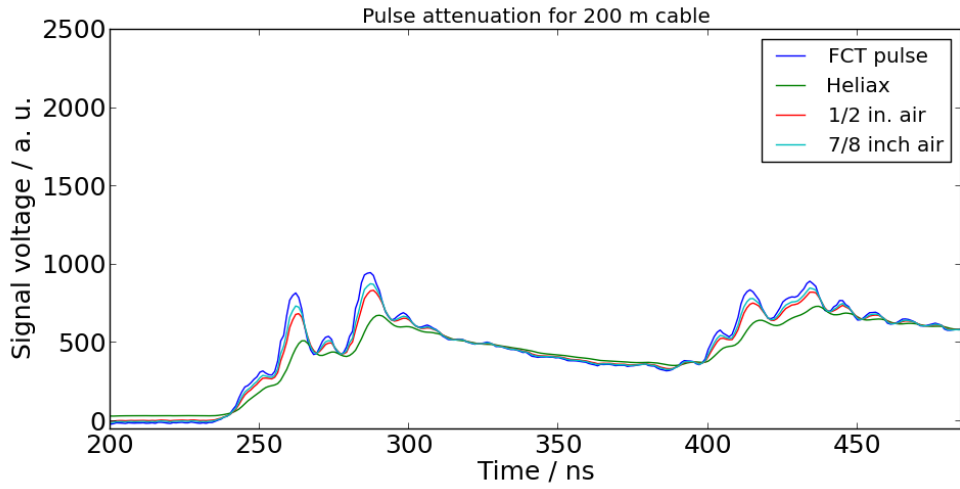


Figure 8: Data for 200 m long cables in Fig. 7 (bottom) for three time intervals.

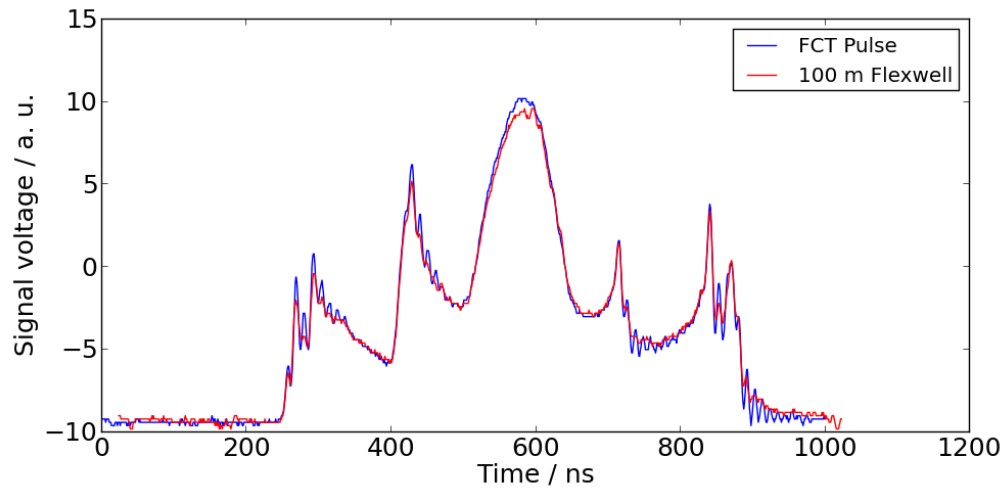


Figure 9: Measured signal distortion in a 100 m long Flexwell coaxial cable.

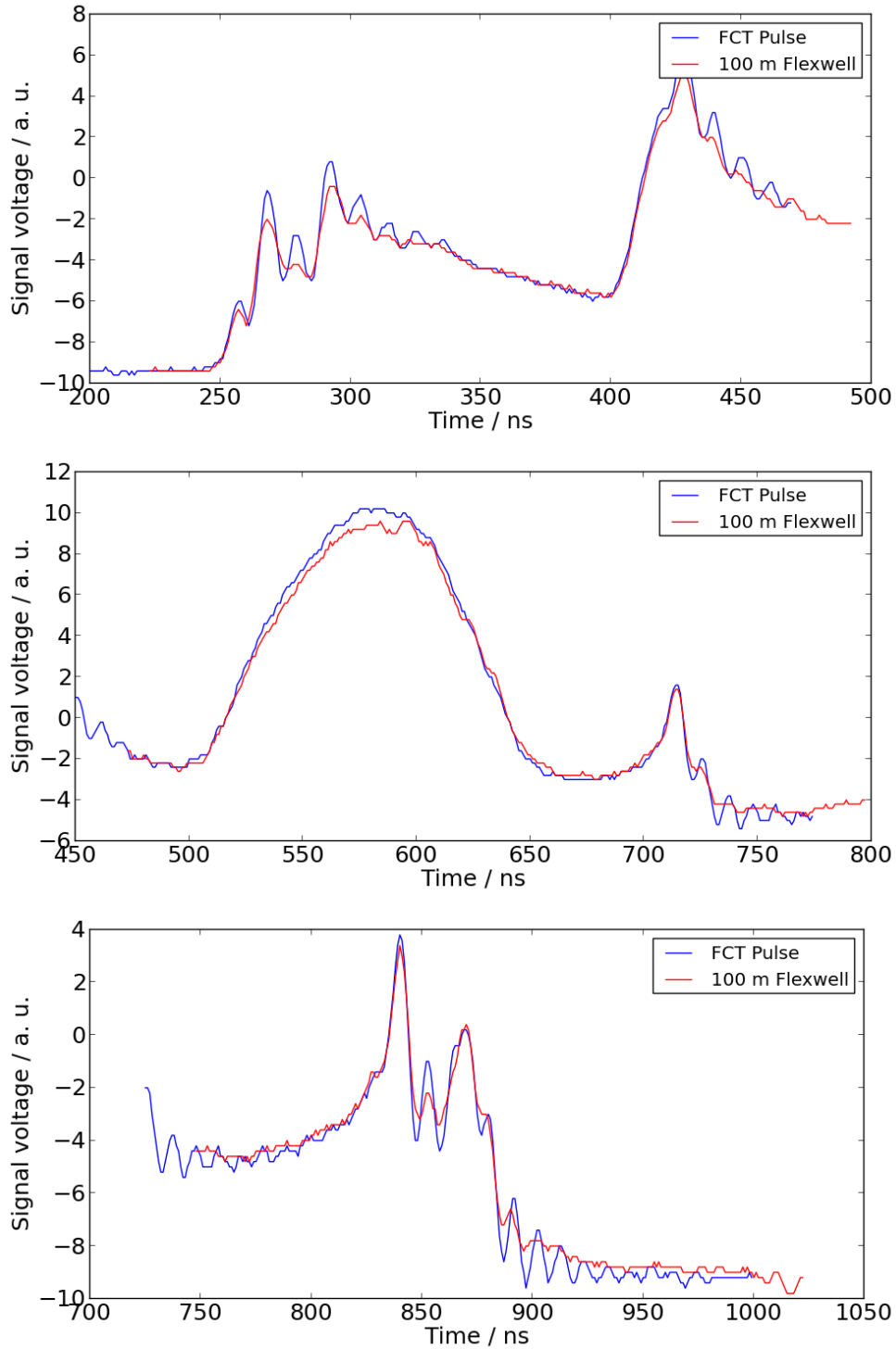


Figure 10: Data for 100 m long cable in Fig. 9 (bottom) for three time intervals. The offset in the two curves is due to the shift in the trigger timing.

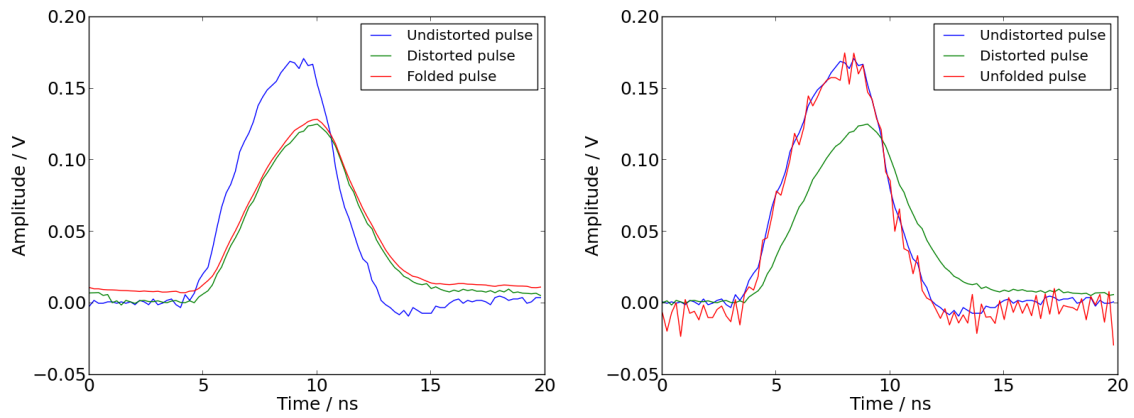


Figure 11: Signal distortion of a 10 ns triangular pulse in Andrew Heliac of 75 m length. Blue trace: pulser signal; green trace: signal at end of transmission line; Red trace: calculated signal by folding (left) the undistorted pulse and unfolding (right) the distorted pulse with the cable response.

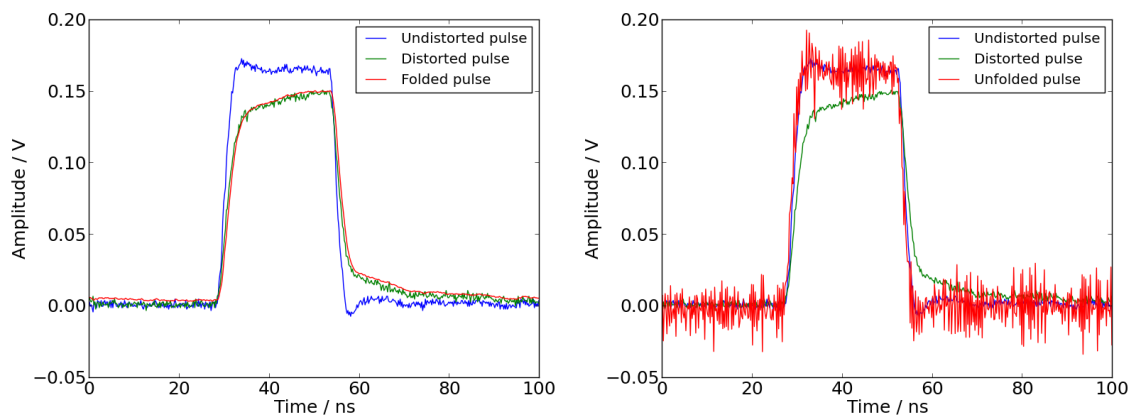


Figure 12: Signal distortion of a 30 ns triangular pulse in Andrew Heliac of 75 m length. Blue trace: pulser signal; green trace: signal at end of transmission line; Red trace: calculated signal by folding (left) the undistorted pulse and unfolding (right) the distorted pulse with the cable response.



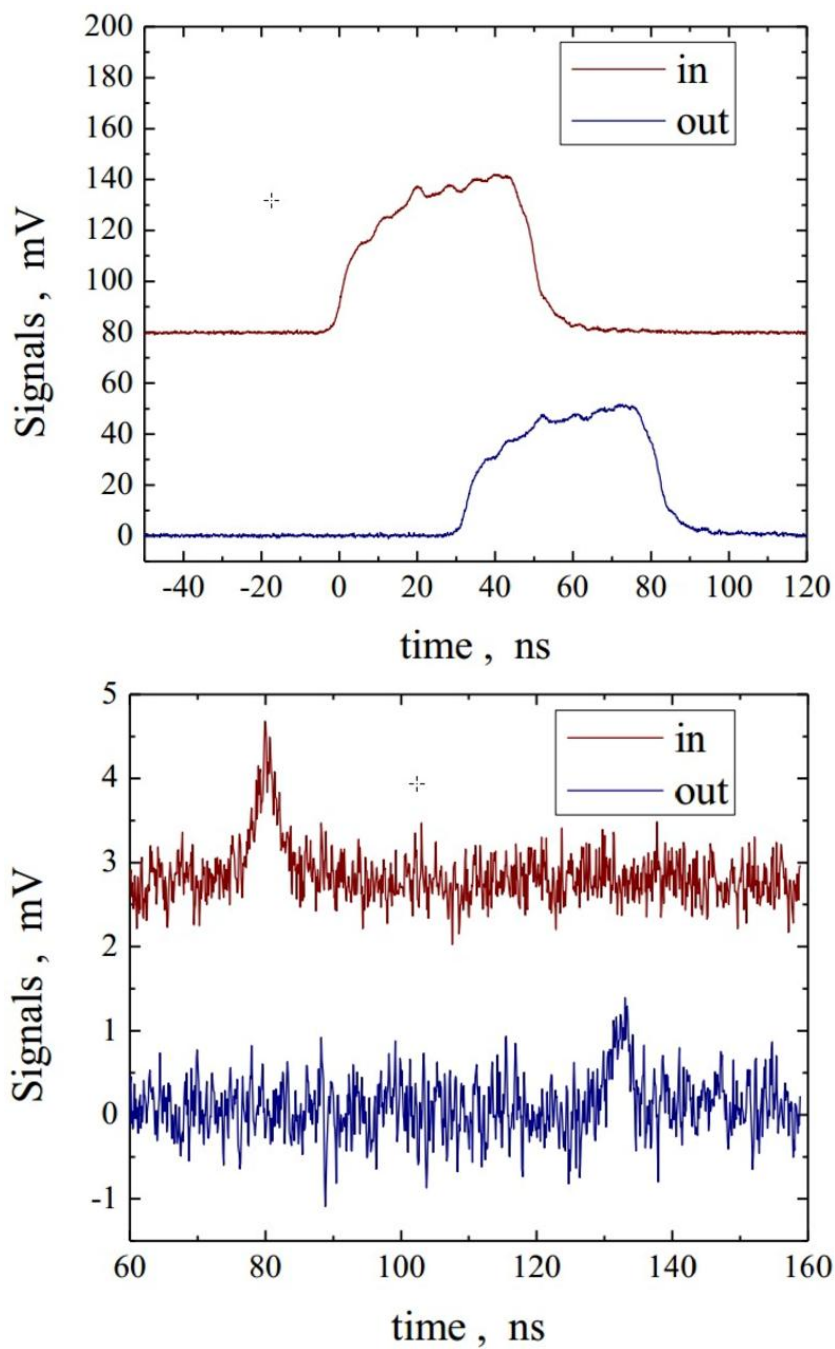


Figure 13: Test of optical link for regular and minimum input voltages. Red = Input pulse to Transmitter; Blue = Output pulse at Receiver. The noise level of the output baseline is about 1.5 mV peak-peak or 0.3 mV(rms).